Supplement of Atmos. Chem. Phys., 16, 4579–4591, 2016
http://www.atmos-chem-phys.net/16/4579/2016/
doi:10.5194/acp-16-4579-2016-supplement

Atmospheric Chemistry and Physics Open Access EGU

Supplement of

Particle water and pH in the eastern Mediterranean: source variability and implications for nutrient availability

Aikaterini Bougiatioti et al.

Correspondence to: Nikolaos Mihalopoulos (mihalo@uoc.gr) and Aikaterini Bougiatioti (kbougiatioti@gmail.com)

Supplementary materials

1. Parameterization between hygroscopic growth factor and RH

Based on the ambient and dry scattering coefficients measured by the two nephelometers, a link between the *f(RH)* and RH is established taking into account all data from the measurement period:

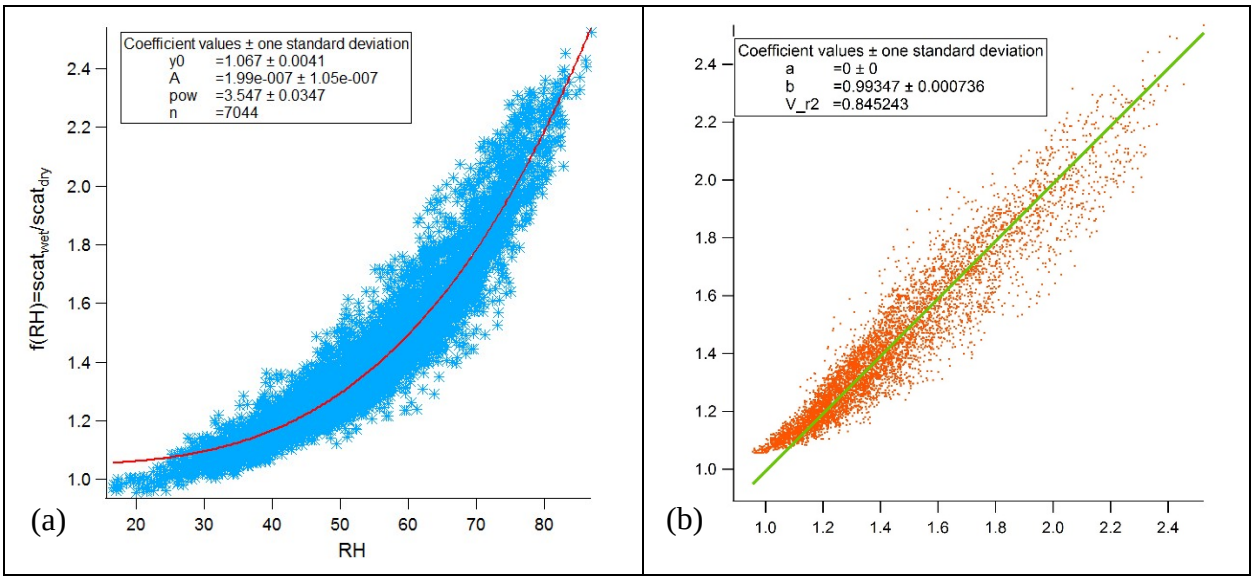

Figure S1: (a) Correlation between *f(RH)* and RH taking into account all available data from the ambient and dry nephelometers, and (b) Correlation between actual and reconstructed *f(RH)* values.

Using the derived parameterization $f(RH) = 1.067(\pm 0.004) + 1.99(\pm 1.05) \cdot 10^{-7} RH^{3.547(\pm 0.035)}$ the reconstruction of the measured hygroscopic growth factor is realized, with values being within 15% of one another.

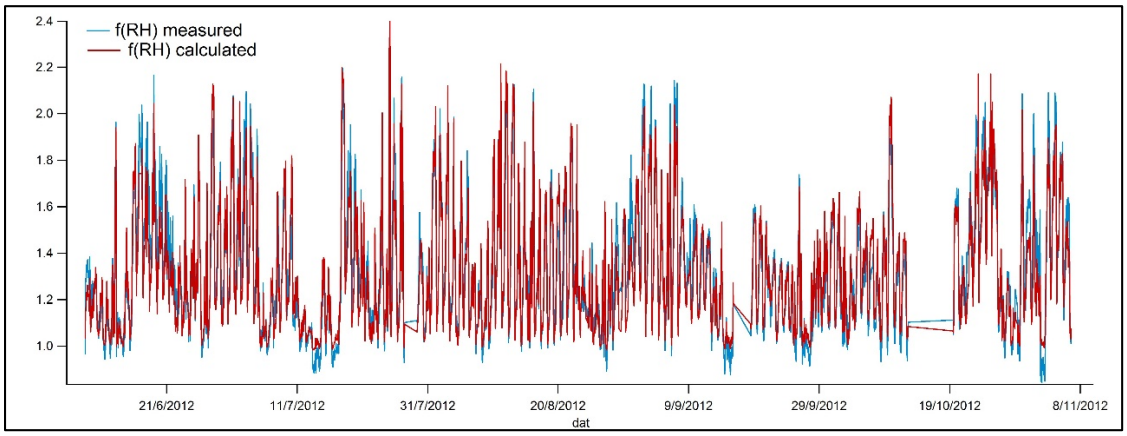

Figure S2: Time series of the measured (blue) and reconstructed (red) hygroscopic growth factors when using solely the dry scattering coefficients and the derived parameterization with the RH.

2. Comparison between ACSM+BC and SMPS-derived submicron mass concentrations

For a period of 2 years, including the sampling period depicted in this study (August-November 2012), the sum of ACSM+BC masses and the submicron mass derived from a scanning particle sizer (SMPS; Tropos-type) were compared, in order to examine the bias introduced by ignoring refractory components other than BC. The particle density for the conversion of volume size distributions to mass from the SMPS, ρ_p, was estimated from the particle composition from the ACSM ammonium, organics and sulfate, using an organic density of 1.35 g cm^{-3} as determined by Lee et al. (2010) for the same site during the summer of 2008 and the density of ammonium sulfate (1.77 g cm^{-3}). The results shown in Figure S3 verify that the bias of neglecting other submicron refractory components is minimum, as also confirmed by size-segregated chemical composition measurements already conducted at Finokalia (e.g. Koulouri et al. 2008).

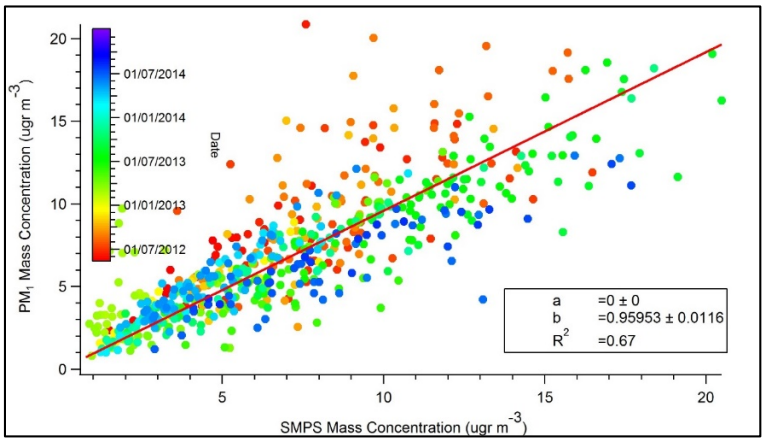

Figure S3: Scatter plot for 2 years of hourly data from the comparison between the PM1 mass derived from the sum of ACSM+BC and the SMPS-derived mass concentration.

3. Uncertainties in calculations by not including gas phase NH_3 to ISORROPIA-II

Finokalia PM1 aerosol contains a considerable amount of sulfates, which does not vary considerably with day for the whole time period considered (June-November 2012), but gas-phase measurements are scarce. Figure S4 represents the diurnal variability of the main non-refractory submicron constituents as measured by the ACSM for the considered measurement period. Furthermore, from long-term measurements of the aerosol -composition at the site, the relative contribution of the main PM_1 constituents, including ammonium, is quite consistent over the years (e.g., Mihalopoulos et al., 1997; Kouvarakis et al., 2001; Sciare et al., 2003; Koulouri et al., 2008, Bougiatioti et al., 2009; 2011; 2013). A fluctuation of 10-20% in sulfate and/or ammonium

concentrations is not expected to be reflected in a pH change, given the logarithmic scale of the property.

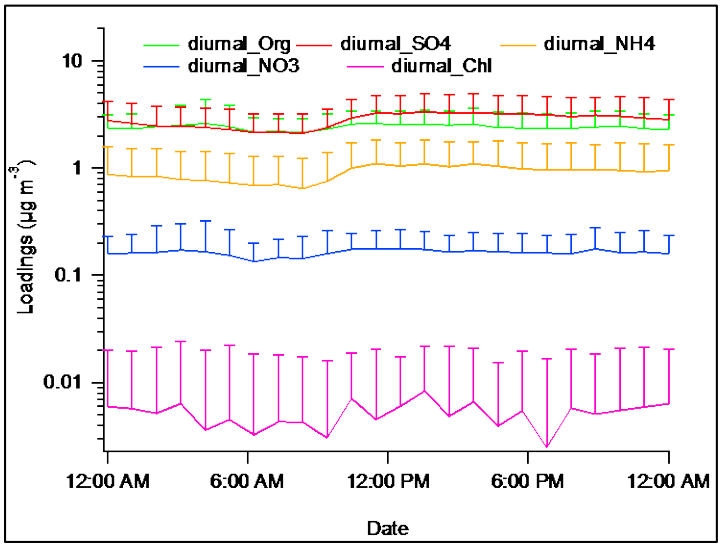

Figure S4: Diurnal variability of the main non-refractory aerosol constituents during the considered measurement period.

In order to assess the uncertainties in our pH calculations by assuming that the sum of NH_3 and NH_4^+ is equal to NH_4^+, i.e. by neglecting the gas phase, we first examined the maximum pH value that can be derived based on the chemical composition measurements. The partitioning of nitric acid between the condensed (NO_3^-) and gas phase (HNO_3) ($\varepsilon(NO_3^-)=NO_3^-/(NO_3^-+HNO_3)$) is derived from ISORROPIA-II by having as input for the model run the average conditions (concentrations, temperature, RH) of the measurement period. Assuming ideal solutions for these conditions and covering a wide range of pH by fluctuating potassium concentration, the resulting partitioning coefficient as a function of pH shows that little nitrate should be present in the aerosol phase when pH is lower than 3 (Figure S5). Indeed, with an average concentration of nitrates of 0.12±0.06 µg m^{-3} in the fine mode and the partitioning coefficient, it is derived that the maximum value of pH that can be observed for the current conditions is 2.

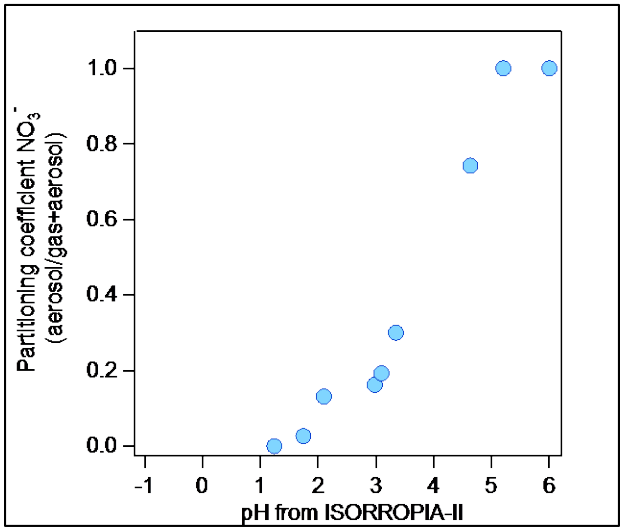

Figure S5: The partitioning of nitric acid between particulate and gas phase as a function of pH for the average conditions during the measurement period.

Furthermore, In order to see the direct influence of not including the gas phase ammonia measurements in the pH calculation, we performed a sensitivity study by adding different amounts of gas phase ammonia to the system and quantifying the response in pH. Initial results of ISORROPIA, the ones that are reported in the manuscript were compared to results obtained after adding 0.5, 1.2, 3.2 and 5 μg m^{-3} of ammonia. The values of 1.2 and 3.2 μg m^{-3} were the median and maximum values of the gas phase measurements respectively. These values are also within the observed values reported by Guo et al. (2015). A lower value (0.5 μg m^{-3}) was also applied and finally 5 μg m^{-3} was selected as an extreme value which is very close to the European critical level for NH_3, established to 8 μg m^{-3} as an annual mean (Air Quality Guidelines for Europe, 2000). From a 3-year study conducted several years ago at the Finokalia station (Kouvarakis et al., 2001) it was seen that $NH_{3(g)}$ concentrations during summertime ranged from 0.02 to 1 μg m^{-3} with a mean and median value of 0.32 and 0.28 μg m^{-3}, respectively, which is well below the maximum selected values for the sensitivity test. Therefore, based on climatology, neglecting the gas phase in the calculations has a difference of around 0.5 units in the pH (from 1.38 to 1.85 median values). Figure S6 shows the different pH median values with the 1st and 3rd percentile as derived for the different amounts of added ammonia. Error bars represent the upper and lower whiskers, derived from the 1st and 3rd percentile and the interquartile range (IQR). It can be seen that by adding even 5 μg m^{-3} of ammonia, pH values differ by a maximum of 1 unit (1.4 vs 2.4), as already mentioned in the manuscript. Results clearly show that neglecting the gas phase NH_3 in the calculations leads to an underestimate of around 0.5 units in the pH (from 1.38 to 1.85 median values) for the NH_3 range reported for Finokalia. This is additional evidence of the weak sensitivity of pH to a wide range of NH_3: the 5-fold increase of added amount of NH_3 causes a unit change in pH, on average.

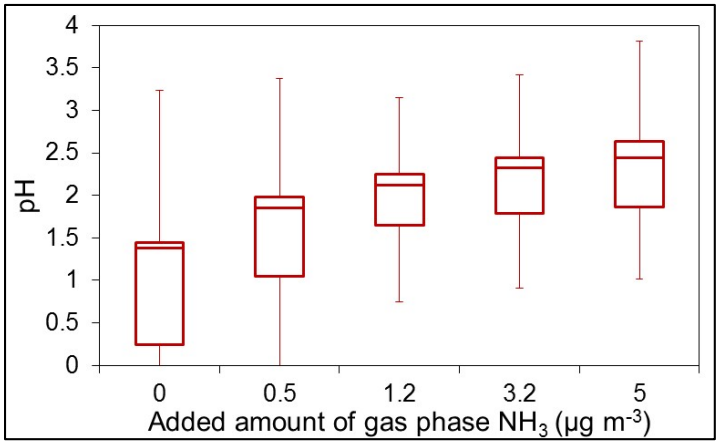

Figure S6: Box plot depicting the median pH values calculated by ISORROPIA II for the different amounts of added gas phase ammonia. Error bars represent the upper and lower whiskers (Q_1-1.5*IQR and Q_3+1.5*IQR, respectively).

4. Diurnal variability of aerosol water and pH of different sources/ source regions

The diurnal variability of the different components of aerosol water and the calculated pH from the thermodynamic model ISORROPIA-II are calculated based on difference sources and source regions in order to see the influence of natural and anthropogenic emissions on both fine aerosol water and pH. Figure S7 portrays the diurnal variability of the water components on the left and the diurnal variability of submicron pH on the right. Sources and source regions are the ones identified in Table 1 of the manuscript, namely biomass burning, Istanbul and countries around the Black Sea, Continental Europe, dust and marine origin.

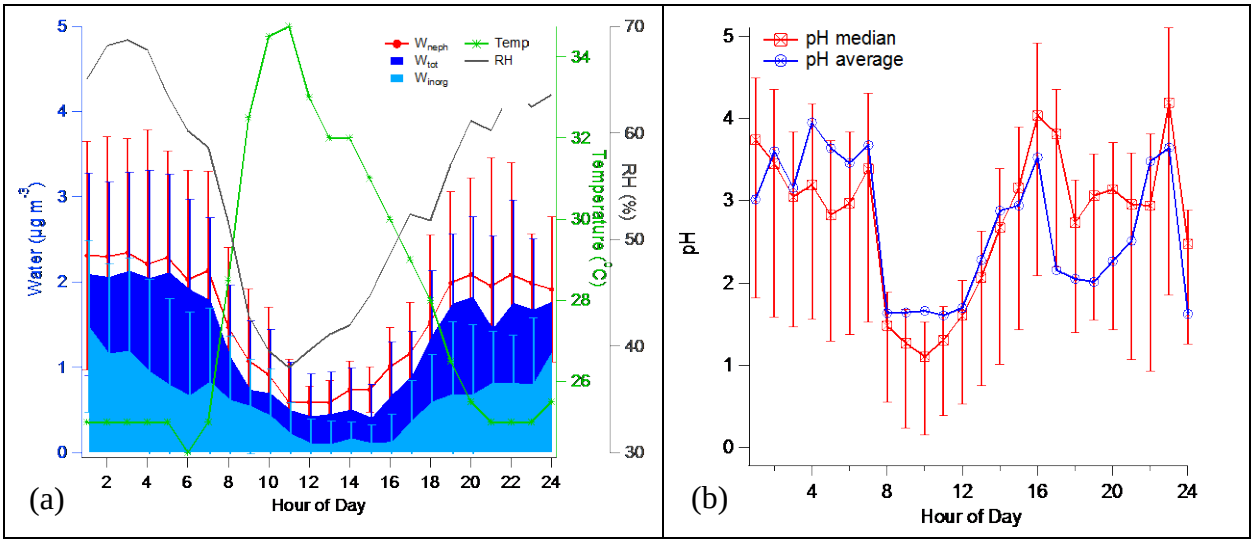

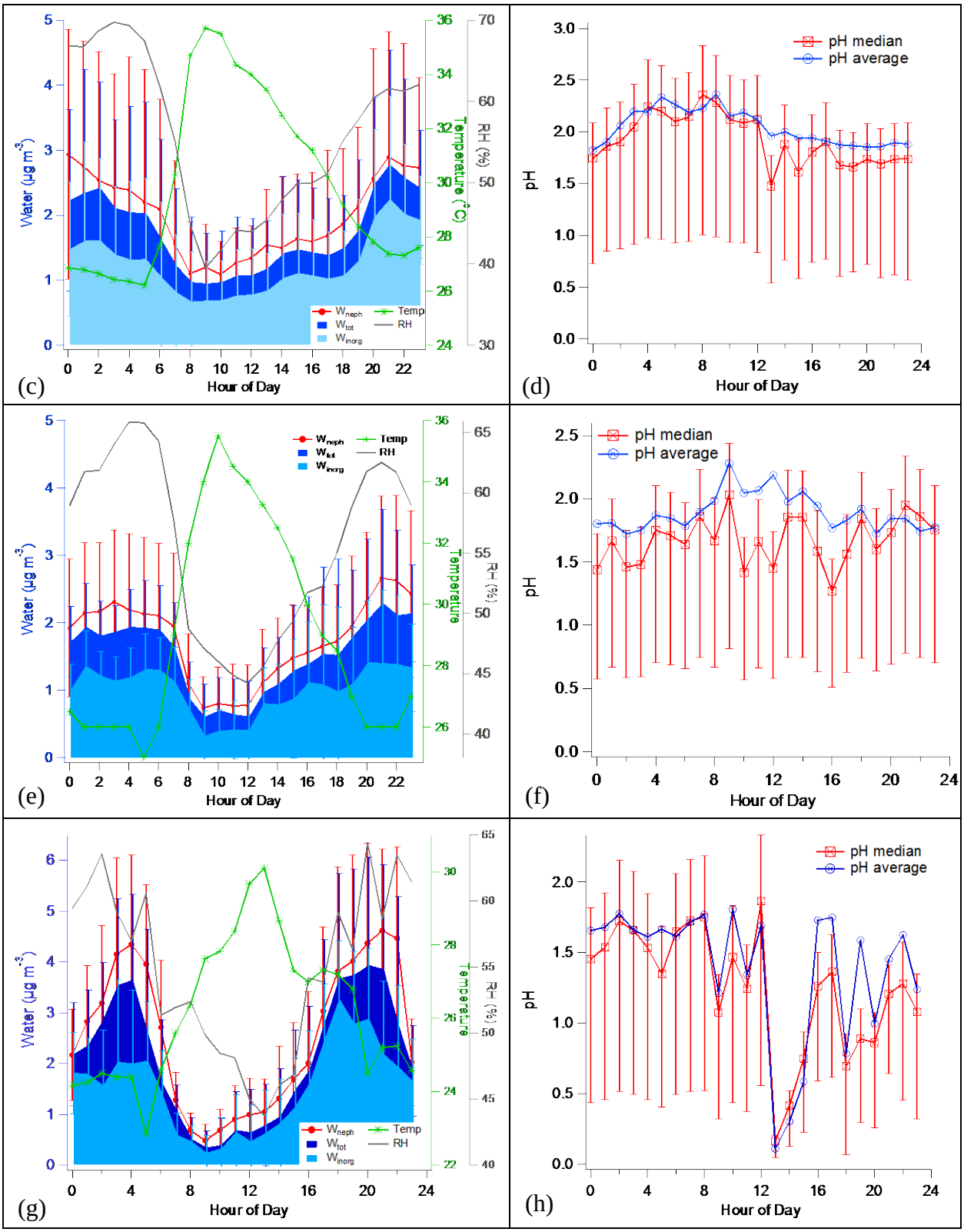
(c)
Water (µg m-3)
Temperature (°C)
RH (%)
Hour of Day
Wneph
Wtot
Winorg
Temp
RH
(d)
pH
pH median
pH average
Hour of Day
(e)
Water (µg m-3)
Temperature
RH (%)
Hour of Day
Wneph
Wtot
Winorg
Temp
RH
(f)
pH
pH median
pH average
Hour of Day
(g)
Water (µg m-3)
Temperature
RH (%)
Hour of Day
Wneph
Wtot
Winorg
Temp
RH
(h)
pH
pH median
pH average
Hour of Day

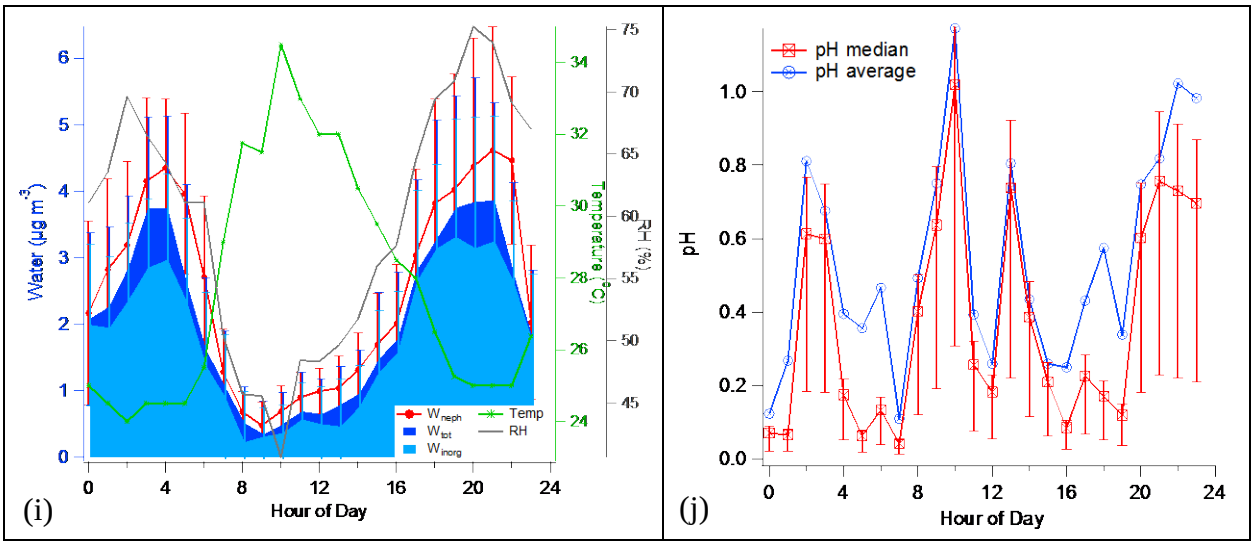

Figure S7: Diurnal variability of aerosol water (left panels) and pH (right panels) for the different sources/source regions: (a) and (b) for biomass burning, (c) and (d) for Istanbul and the Black Sea region, (e) and (f) for Continental Europe, (g) and (h) for mineral dust, and (i) and (j) for marine origin.

5. Back trajectory analysis

Based on the back trajectory analysis performed for the identification of the different types of sampled aerosol, a representative plot for each category type as depicted also just above is provided in Figure S8.

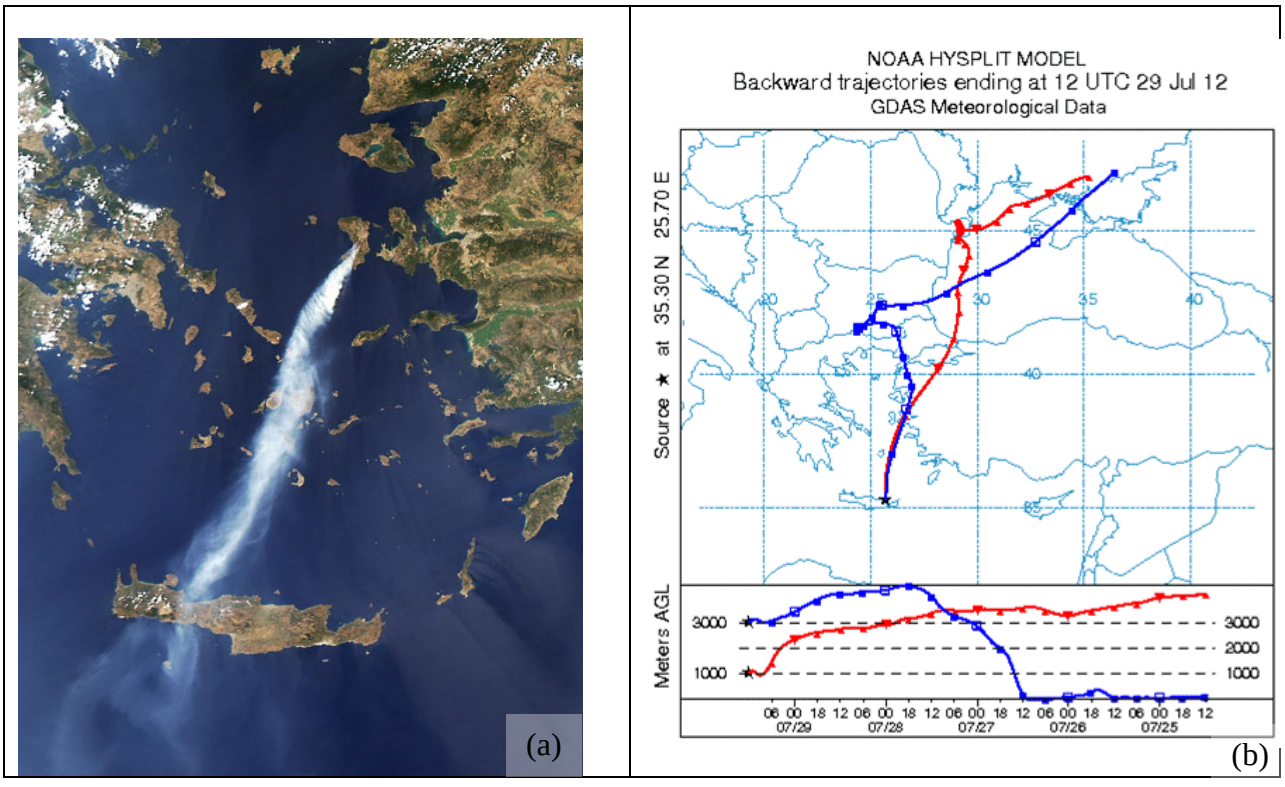

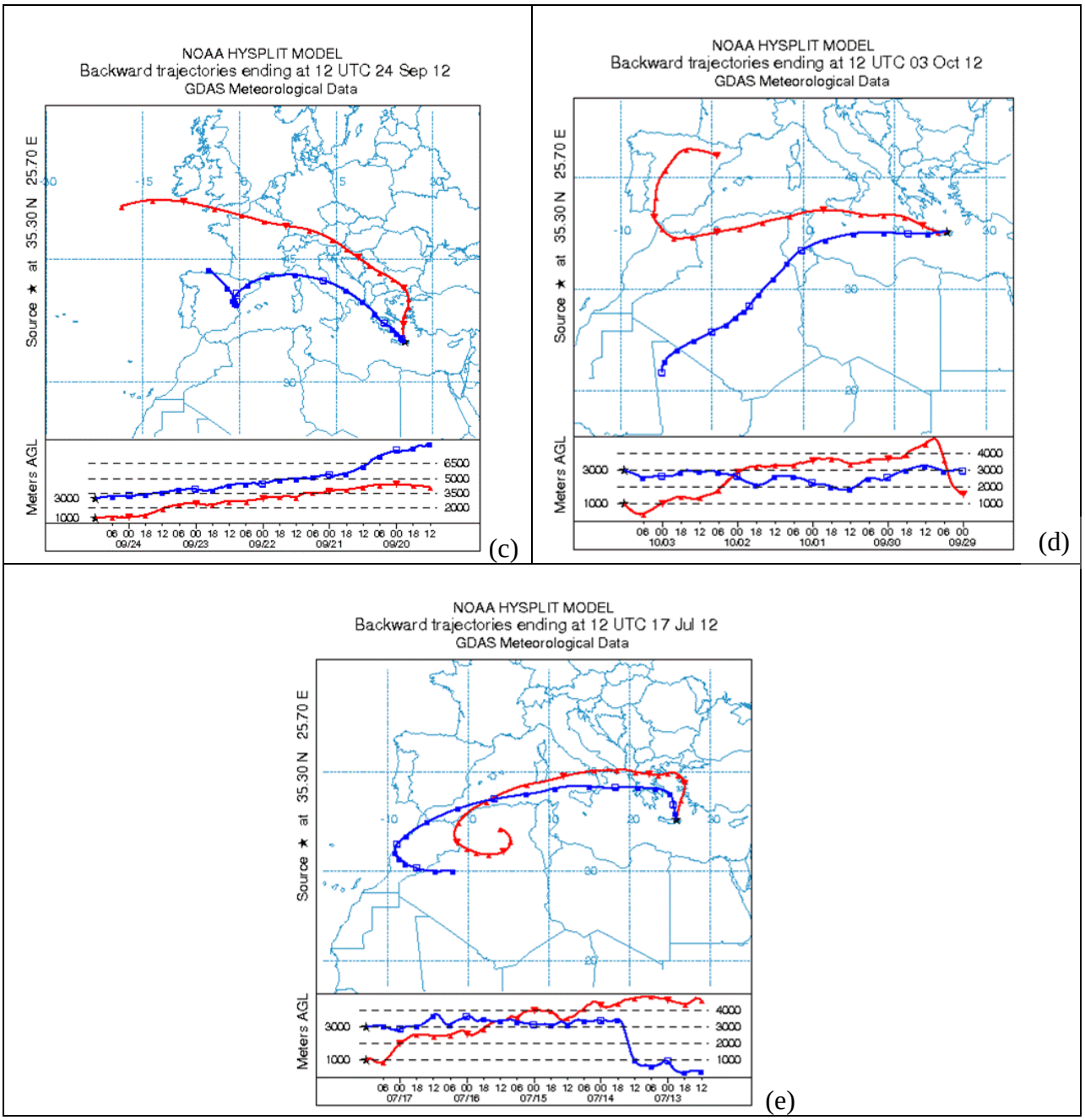

Figure S8: Back trajectory analysis provided by HYSPLIT model for the different sources/source regions: (a) for biomass burning (MODIS image), (b) for Istanbul and the Black Sea region, (c) for Continental Europe, (d) for mineral dust, and (e) for marine origin.